Domenech-Carbo, A.; Domenech Carbo, MT.; Ferragud-Adam, X.; Ortiz-Miranda, AS.; Montoya, N.; Pasies -Oviedo, T.; Peiró-Ronda, MA.... (2017). Identification of vegetal species in wooden objects using in situ microextraction-assisted voltammetry of microparticles. Analytical Methods. 9(13):2041-2048. doi:10.1039/c7ay00323d

Identification of vegetal species in wooden objects using *in situ* microextraction-assisted voltammetry of microparticles

Antonio Doménech-Carbó*[a], María Teresa Doménech-Carbó[b], Xavier Ferragud-Adam[a,b], Annette S. Ortiz-Miranda[b], Noemí Montoya[a], Trinidad Pasíes-Oviedo[c], María Amparo Peiró-Ronda[c], Jaime Vives-Ferrándiz[c], Yolanda Carrión-Marco[d,e]

[a] Departament de Química Analítica. Universitat de València. Dr. Moliner, 50, 46100 Burjassot (València) Spain.
[b] Institut de Restauració del Patrimoni. Universitat Politècnica de València. Camí de Vera 14, 46022, València, Spain.
[c] Museu de Prehistòria de València. Corona 36, 46003, Valencia, Spain.
[d] Departament de Prehistòria i Arqueologia, Facultat de Geografia i Història, Universitat de València, Av. Blasco Ibañez 28, 46010 Valencia, Spain.
[e] PREMEDOC (GIUV2015-213) Prehistoria del Mediterráneo Occidental.

* Corresponding author, e-mail: antonio.domenech@uv.es.

ABSTRACT:

A method for identifying the vegetal species in wooden objects using microextraction-assisted voltammetry of microparticles is described. The proposed methodology, aimed to facilitate tasks of patrimony conservation, is based on the record of the voltammetric response of microparticulate films of compounds resulting from micro extraction with organic solvents (ethanol, acetone, chloroform) of micro- or sub-microsamples of wood in contact with aqueous buffers. Upon application of bivariant and multivariant chemometric techniques, the obtained voltammetric responses led us to identify different taxonomic groups from the characteristic voltammetric profiles. Application to a series of samples of cultural heritage wooden objects from different European and American provenances dated to *ca*. 375-350 BC and to historical periods, 14th, 17-19th century, is described.

KEYWORDS: Heritage; Wooden objects; Vegetal families; Voltammetry of microparticles; Chemometric techniques.

1. Introduction

The identification of vegetal species in wooden objects of cultural heritage, namely, sculptures, altarpieces, coffered ceilings, furniture, hardware, etc. is an important analytical target in the fields of heritage conservation and archaeometry.[1] Traditionally, this objective was achieved by anthracology, consisting of the botanical identification of the wood samples on the basis of their anatomy via microscopy examination of sections of wood samples.[2,3] Wood can be often identified to the species range, but anatomical similarities between groups of species can limit identification to the genus or family range, or even larger groups (e.g. Conifer/Angiosperm). The range of identification often depends on the quality of the sample (conservation, size) as well. Thus, frequently is used the concept of "taxon", equivalent to an identification unit, regardless of the degree of detail reached.[4]

Anthracological analysis, which is supported by microscopy techniques,[5-7] can be subsequently correlated to radiocarbon dating for archaeological purposes.[8] Other techniques have been recently applied to the identification of wood remains, namely, synchrotron X-ray microtomography,[9] gas chromatography/mass spectrometry[10-12] and solid-state nuclear magnetic resonance[13,14] techniques, among others.[15]

Genetic analysis including DNA barcoding methodologies,[16-18] based on DNA sequencing after non-destructive extraction can also be applied, in favorable cases, for studying ancient vegetal matter.[10,19] Chemotaxonomy, the method of biological classification based on the chemical composition of living organisms, can be based on a variety of compounds, from proteins, carbohydrates fatty acids, aldehydes, primary and secondary alcohols, ketones, long-chain alkanes, alkyl esters, triterpenoids, tocopherols, or aromatic compounds.[20] The chemical composition of wood, in particular, polyphenolic compounds,[21] was early used for chemotaxonomic purposes.[22] In particular, lignins, natural polymers from oxidative coupling of 4-hydroxyphenyl-propanoids,[23] exhibit a considerable variety because of the plasticity of the combinatorial polymerization reactions.[24]

Here, we report a simple electrochemical methodology for identifying vegetal species in wooden objects of cultural heritage based on the record of the electrochemical response

of the polyphenolic components of the wood. This method, which exploits the capability of organic solvents for extracting polyphenolic compounds from vegetal matter,[25] is based on the record of the voltammetric response of a microparticulate film (formed on the surface of an inert electrode from the polyphenolic components extracted from a micro- or sub-microsample of wood) in contact with aqueous buffers after *in situ* microextraction-assisted voltammetry of microparticles (VMP) assay. VMP is a technique developed by Scholz et al.[26] which provides analytical information on sparingly soluble solids.[27,28] This technique has been previously applied in the field of patrimony conservation.[29,30] Much polyphenolic compounds in wood can produce a well-defined electrochemistry in solution-phase, from lignins[31-33] to flavonoids, flavones, etc.[34-37] and solid state.[38-45] This solid state electroanalytical methodology has also been applied to study the antioxidant capacity of tea leaves[46] and other vegetables[47] as well as for screening vegetal varieties.[48,49]

The proposed methodology permits to identify vegetal families and species from the chemometric analysis of the recorded voltammetric pattern without the need for identifying and quantifying the individual compounds present in the sample. In order to study the possibility of *in situ* or out-lab measurements, VMP experiments were conducted in non-degasified aqueous acetate buffer using laboratory and portable equipments. The method has been applied to samples of ca. 1 μg extracted from wooden objects which remained under an atmospheric environment; i.e., which do not suffered carbonization nor undergo exigent conditions of aging such as burial conditions or sub-aquatic storage, the samples consisting of a set of wood fragments from objects of different provenances dating back to *ca*. 375-350 BC and to historical periods, 14th, 17-19th centuries. Wood species identification was validated using microscopy examination of samples prepared in the three anatomical sections of wood (cross, tangential and radial). Complementary HPLC/MS experiments were performed on ethanolic extracts of wooden samples.

2. Experimental

2.1. Materials, instrumentation and procedures

Rutin, quercetin, morin, catechin and chlorogenic acid were purchased from Sigma-Aldrich (Madrid, Spain) and Quercetin-3-rutinoside from Merk (Darmstadt, Germany). Aqueous acetic acid/sodium acetate buffer solutions in concentration 0.25 M and pH 4.75 and 0.10 M potassium phosphate buffer at pH 7.0 were used as supporting electrolytes for electrochemical measurements using nanopure water and reagents from Panreac (Barcelona, Spain). In order to test the possibility of in field measurements using available portable equipments, no degasification of the electrolyte was carried out.

Wood samples, consisting of needles of ca. 0.5 mm length, were taken from the inner region of the different archaeological objects with the help of a microscalpel. The provenance and main characteristics are summarized in Table 1. A series of wood specimens from the repository of the Institut de Restauració del Patrimoni of the Universitat Politècnica de València were taken as reference materials. These include woods from trees of the Fagaceae (*Quercus*, *Castanea* and *Fagus* genera), Juglandaceae (*Juglans*), Ulmaceae (*Ulmus*), Sapindaceae (*Acer*), Salicaceae (*Populus*, *Salix*), Oleaceae (*Olea*, *Fraxiunus*), Pinaceae (*Pinus*, *Cedrus*), Cupressaceae (*Juniperus*, *Cupresus*), Taxaceae (*Taxus*) and Buxaceae (*Buxus*) families which cover the main species used in the Mediterranean area for architectural and decorative purposes and/or in furniture and/or as panels for painting. The detailed list of species is presented as Supplementary information (Table S1).

Electrochemical experiments were performed at 298 ±1 K in a CH cell using either a laboratory CH I660 potentiostat (Cambria Scientific, Llwynhendy, Llanelli UK) or Ivium CompactStat portable equipment (Ivium Technol. B.V., Eindhoven, The Netherlands). A BAS MF2012 glassy carbon working electrode (GCE) (geometrical area 0.071 cm^2), a platinum wire auxiliary electrode and an Ag/AgCl (3M NaCl) reference electrode were used in a typical three-electrode arrangement. Voltammetric measurements were performed with a freshly-prepared sample-modified GCE. For electrode conditioning, the wood fragment was macerated in an agate mortar adding 0.5 mL of the organic solvent during 2 min. 50 μL of the resulting suspension were dropped onto the GCE surface. After solvent evaporation in air, the electrode was inserted into the electrochemical cell and electrochemical runs were performed. HPLC grade ethanol, acetone and chloroform (Carlo Erba) were used for extractions. Linear potential scan (LSV), cyclic voltammetry (CV) and square wave voltammetry (SWV) were used as detection modes.

The chromatograms of specimens were performed in an AB SCIEX TripleTOF™ 5600 LC/MS/MS System. The date acquisition used are in negative mode, over a mass range of 100 – 950 m/z. Automated calibration was performed using an external calibrant delivery system (CDS) which infuses calibration solution prior to sample introduction. The MS was using an IDA acquisition method with: the survey scan type (TOF-MS) and the dependent scan type (product ion) using -30V of collision energy. Data was evaluated using the qualitatively evaluated using the PeakView™ software.

2.2. Samples

Wood samples were examined with a light microscope Leica DM2500 P (Leica Microsystems, Heidelberg, Germany). The amount of wood needed for identification under microscope is variable, depending on the challenges cited above, but it can generally be enough with a few mm^3 of well oriented wood. When analyzing wooden workpieces, we try to sample in an inconspicuous area.[5] In the case of wood from altarpieces, needles of ca. 0.5 mm length were obtained from the inner parts of the piece when exposed (see Figure 1a), avoiding wooden surfaces usually covered by ground layers (see Figure 1b). Wood identified in this study by anatomical observation was exclusively not carbonized wood but due to the small amount of sample available and its state of conservation, it was often difficult to obtain satisfactory radial sections as can be seen in optical microscopy images under diascopic illumination and parallel polarized light of the radial section of samples **S7** (Figure 1c) and **S6** (Figure 1d), where large pinoid pits occupied practically the entire cross-field.

We have sampled only some wood fibers bonded to metal objects in the case of the Iron Age site of La Bastida de les Alcusses (Moixent, Spain), and small samples of three wooden sculptures from the church of San Cristobal Mártir (Picassent, Spain), enough to obtain relevant results. In these cases, the degree of identification achieved was not dependent on sample size, but on wood preservation since, as mentioned above, not carbonized wood is frequently altered by natural biodegradation processes. The microstructure of wood sections was observed by using field emission scanning electron microscopy (FESEM) (Model S-4800, Hitachi Ltd., Tokyo, Japan) operating at 20 kV.

The specimens were fixed with carbon tape on the holder and gold-coated using conventional protocols, as already described.[5]

3. Results and discussion

3.1. General voltammetric pattern

Figure 2 shows the cyclic voltammograms, after semi-derivative convolution, of microparticulate films prepared from the ethanol and acetone extracts of *Quercus robur* in contact with aqueous acetate buffer at pH 4.75. Upon scanning the potential from 0.0 V vs. Ag/AgCl in the positive direction, a series of anodic peaks appear between ca. +0.2 to ca. +1.2 V (A_{pp}). These peaks, as judged upon comparison with the voltammograms for microparticulate deposits of quercetin, rutin, morin, catechin and chlorogenic acid, reference compounds,[46-49] can be attributed to the oxidation of polyphenolic compounds. This assignment is also in agreement with the reported solution phase electrochemistry of lignins[31-33] and flavonoids,[34-37] as well as the solid state electrochemistry of different phenolic compounds.[38-45] In the subsequent cathodic scan, the voltammogram is dominated by the prominent signal for the reduction of dissolved oxygen (C_{ox}) because, as previously noted, non-degasified electrolytes were used in order to test the possibility of in field measurements using portable equipments. Interestingly, the voltammetric profile varied from one wood species to another and was also dependent on the solvent used for the microextraction and the electrolyte.

Replicate experiments at freshly prepared electrodes produced well-defined responses with high degree of similarity. Repeatability tests were performed using: i) three independently prepared deposits of each one of the studied extracts on the same glassy carbon substrate electrode and ii) three independently prepared deposits of each one of the wood extracts on different substrate electrodes. In all cases, peak potentials were reproduced with a maximum dispersion of ±10 mV whereas the voltammetric pattern (in terms of current ratios relative to the maximum peak current) remained within a 5-10% of relative standard deviation. Cyclic and square wave voltammograms (see Supplementary materials, Figures S1 and S2) also provided species-characteristic voltammetric profiles. Linear scan voltammograms submitted to semi-derivative deconvolution were selected for species identification as a result of the compromise between peak resolution and repeatability.

3.2. Chemical and electrochemical fingerprints

HPLC/MS analysis of ethanolic extracts of wood samples evidenced the presence in the same of a considerable variety of compounds, as can be seen in Figure 3 where the chromatograms of ethanolic extracts of *Quercus robur* and *Prunus avium* are shown. Interestingly, a variety of polyphenolic compounds were identified in such samples, namely, baicalein, 6-geranylnaringenin, 7-hydroxysecoisolariciresinol, prodelphinidin dimer B3, trans-ferulic acid, dihydroquercetin, hesperetin, luteolin, nepetin, trans-ferulic acid, among others listed as a Supplementary information (Table S2).

Although the studied samples have in common several compounds (nepetin and trans-ferulic acid), there are different chemical fingerprints able to characterize the different species. This is in agreement with the recognized use of several compounds (typically, terpenoids for Pinaceae) as chemosystematic markers.[50-52] The complexity of the composition of wood extracts and the inherent difficulty in solving chromatographic profiles such as in Figure 3, make potentially interesting the use of complementary techniques able to be applied for identification purposes.

The possibility of obtaining electrochemical fingerprints identifying different vegetal species from woods is illustrated in Figure 4 where linear scan voltammograms, after semi-derivative deconvolution, of ethanolic extracts from specimens of different taxonomic groups: a) *Ulmus glabra* (Urticales, Urticaceae), b) *Quercus petrae* (Fagales, Fagaceae), c) *Taxus baccata* (Pinales, Taxaceae) and d) *Prunus avium* (Rosales, Rosaceae) are shown. One can see in this figure that, after semi-derivative convolution, the extracts of the different species provide clearly different voltammetric patterns in the region of potentials between 0.0 and +1.20 V where the oxidation of polyphenolic compounds occurs. The specificity of the voltammetric response is maintained using acetone and chloroform extracts. Interestingly, one can define common voltammetric patterns for the different families whereas the differences between genera and species are in general lower (*vide infra*).

The A_{pp} anodic processes at potentials ca. +1.0 V were in general highly irreversible, with no coupled cathodic signals even at relatively high potential scan rates (10^3 mV s^{-1}), a feature compatible with the electrochemistry of lignins,[31-33] whose oxidation is represented in Figure 5a for syringic acid, a compound representative of one of the main structural subunits of lignins. Available data on the electrochemistry of natural polyphenolic compounds,[31-45] suggest that the A_{pp} processes appearing at relatively low potentials (between +0.2 and +0.6 V) may, in principle, be assigned to the two-electron, two-proton oxidation of the o-catechol units (as a typical example, the oxidation of the 3',4'-dihydroxybenzoic moiety of flavonoids, see Figure 5b for baicalein) yielding the corresponding *o*-quinone(s), whereas the oxidation peaks at more positive potentials can be attributed to the oxidation of other phenolic motifs.[34-45]

3.3. Wood identification in samples.

The relevant point to emphasize is that the ethanolic, acetone and chloroform extracts of the studied woods were characteristic of the different taxonomic groups. Application of voltammetric records for identification purposes in archaeological remains required the maintenance of the electrochemical response regardless their aging and possible deterioration. Figure 6a shows the FESEM image of a radial section of sample **S11** from the church of San Cristóbal Mártir (Picassent, Spain), showing characteristic pitting of tracheids allowing to identify it as *Pinus* tp. *halepensis*. Figure 6b compares the voltammograms of microparticulate deposits from ethanolic extracts of a contemporary specimen of *Pinus halepensis* (black) and samples **S11** (red) and **S14** (green**)**, this last dated back *ca*. 375-350 BC. The close similarity between such voltammograms permits to identify the above species in such samples. These differ slightly but significantly from the voltammograms of *Taxus baccata* (black) and sample **S10** (red) from the San Cristobal Mártir church (Picassent, (Spain), 18^{th}-19^{th} century) in Figure 6c and those in Figure 6d for *Pinus sylvestris* (black), sample **S6** (red, from the altarpiece of the *Verge de Gràcia* at the *Sant Miquel Arcángel* church of Enguera, (Spain), authored by Paolo de San Leocadio, 1482-1484) and sample **S7** (green, from *Taules de Sant Vicent* in the altarpiece of the *Sant Jaume* church of Algemesí, (Spain), painted by Francisco Ribalta, 1603-1605), thus permitting the corresponding species attribution.

In order to define quantitative pattern recognition criteria, it has to be accounted that there is no possibility of a precise control of the amount of sample transferred onto the electrode surface so that the currents varied in replicate experiments. Accordingly, normalized voltammograms were constructed, in line with Wang et al.,[53] taking the ratio between the current at a given potential, $i(E)$, and the maximum current, $i(\max)$, vs. the applied potential E. On first examination, two-dimensional diagrams plotting the normalized current at a potential E, $I(E) = i(E)/i(\max)$, at two selected potentials results in grouping of experimental data points allowing for a discrimination at the taxonomic level of families (see Figure 7). Accordingly, the identification of wood taxonomic groups can, in principle, be achieved without need of a detailed analysis of the chemical composition of the extracts.

The distinction between different species of the same genus, however, can present more difficulties, as illustrated in Figure 8 where the voltammograms recorded for samples **S1** and **S3** are compared with those of *Quercus robur* and *Quercus pyrenaica* contemporary specimens, respectively. Although examination of such voltammograms suggested the assignment of such samples to the respective *Quercus* species, it is convenient to establish refined criteria for species discrimination.

For this purpose, chemometric methods can be applied.[53] Following prior studies for leaf extracts of plants,[54,55] taking current values at n potentials, normalized current data provide a matrix of $(1 \times n)$ dimensions which can be converted into a matrix of $(m \times n)$ dimensions combining the data for extracts in m different solvents and/or electrolytes. Then, multivariate chemometric methods can be applied for electrochemotaxonomic purposes correlating electrochemical cluster analysis with phylogenetic trees.[54,55] The same set of electrochemical data can be used for identification purposes upon determining the degree of matching between the voltammogram of the samples and the reference woods. Using the normalized voltammograms previously described (where $0 \leq I(E) \leq 1$), the degree of matching between two series of voltammograms for two specimens A and B can be approached by a *f*-coefficient defined as:

$$f = 1 - \sqrt{\frac{\sum_{j=1}^{m}\sum_{k=1}^{n}\left[I_{jk}(E_k)_A - I_{jk}(E_k)_B\right]^2}{n+m}} \qquad (1)$$

Graphically, the degree of matching can be examined using bi- and tridimensional diagrams combining the corresponding set of $I(E)$ data. Examples of two different levels of matching are illustrated in Figure 9, where representations of the LSVs of ethanolic extracts of sample **S3** in contact with acetate buffer are compared with those for *Quercus robur* and *Fagus sylvatica*. In the case of perfect matching, plots of $I(E)_A$ vs. $I(E)_B$ should be a straight line passing by the origin and slope 1.0. As can be seen in Figure 9a, the representation for A = *Quercus robur*, B = sample **S3** is close to that expectance. In contrast, the same representation for A = *Fagus sylvatica*, B = sample **S3** (figure 9b) clearly diverges from the aforementioned line of perfect matching. Table 1 summarizes the taxonomic units identified for archaeological wood samples in this study based on anthracological and electrochemical methodologies where an excellent agreement between them was obtained. For practical purposes, we imposed as a condition for electrochemical matching $f > 0.95$.

Another graphical indication of the degree of matching can be obtained by plotting the values of the square of the differences between the normalized currents at each potential, $[I(E)_A - I(E)_B]^2$ vs. E. As can be seen on comparing the corresponding representations in Figures 9c and 9d, the differences between sample **S3** and *Quercus robur* are considerably lower than the differences between the same sample and *Fagus sylvatica*.

It is pertinent to note, however, that the most reasonable assignment can be made only at the level of genera or family. The assignment of a concrete species can be in most cases difficult because: i) the similarity in the voltammetric response of closely related species, ii) the use of local species or varieties without contemporary documented equivalents, and, iii) the possibility of differences in sample deterioration and/or aging under environmental conditions. Our data suggest that there is possibility of subtle changes in the voltammetric response of a given species upon aging, but this aspect, which is under investigation, involves the disposal of a much more extensive set of samples for properly testing it. In spite of these limitations, the proposed approach can

be considered as a plausible methodology complementing the existing analytical techniques of identification of vegetal species in wooden objects in order to facilitate their study and conservation.

4. Conclusions

Microparticulate films deposited on glassy carbon electrodes from ethanolic, acetone and chloroform extracts of wood microsamples provide well-defined voltammetric responses in contact with aqueous electrolytes. Such responses consist mainly of oxidation signals which can be associated to the oxidation of flavones, flavonols, lignins and other polyphenolic components of wood. The recorded voltammograms were highly characteristic of the vegetal species and are usable for characterizing different taxonomic groups.

The application of this methodology in the field of heritage and conservation studies is illustrated by the identification of woods from a series of samples from furniture, weapons and sculptures dated to *ca*. 375-350 BC and to historical periods, 14^{th}, $17\text{-}19^{th}$ century. Due to its simplicity and accessibility, the proposed methodology can be potentially usable as a complementary tool of existing techniques of identification usable in archaeometry and conservation of cultural heritage.

Acknowledgements

Financial support from the MICIN Projects CTQ2014-53736-C3-1-P and CTQ2014-53736-C3-2-P, which are also supported with ERDF funds, is gratefully acknowledged. Thanks to the Museum of Prehistory of Valencia, especially to the director Helena Bonet.

REFERENCES

1 J. M. Madariaga, *Anal. Methods* 2015, **7**, 4848–4876.

2 F. H. Schweingruber, *Anatomy of European woods*. Hupt, Stuttgart, 1990.

3 B. T. Nigra, K. F. Faull and H. Barnard, *Anal. Chem*. 2015, ***87***, 3–18.

4 J. –L. Vernet, P. Ogereau, I. Figueiral, C. Machado Yanes and P. Uzquiano, *Guide d'identification des charbons de bois préhistoriques du sud-ouest de l'Europe*. CNRS, Paris, 2001.

5 Y. Carrión and P. Rosser, *Antiquity* 2010, **84**, 747–764.

6 M. Moskal-del Hoyo, *J. Archaeol. Sci*. 2012, **39**, 3386–3395.

7 F. Ruffinatto, C. Cremonini, N. Macchioni and R. Zanuttini, *J. Cult. Herit*. 2014, **15**, 614–620.

8 J. –L. Vernet, E. Bazile and J. Evin, *Bull. Soc. Préhist. Fr*. 1979, **76-3**, 76–79.

9 S. Mizuno, R. Torizu and J. Sugiyama, *J. Archaeol. Sci*. 2010, **37**, 2842–2845.

10 M. F. Deguilloux, L. Bertel, A. Celant, M. H. Pemonge, L. Sadori, D. Magri and R. J. Petit, *J. Archaeol. Sci*. 2006, **33**, 1216–1227.

11 E. W. H. Hayek, P. Krenmayr, H. Lohninger, U. Jordis, W. Moche and F. Sauter, *Anal. Chem*. 1990, **62**, 2038–2043.

12 P. F. Van Bergen, I. Poole, T. M. A. Ogilvie, C. Caple and R. P. Evershed, *Rapid Commun Mass Spectr*. 2000, **14**, 71–79.

13 M. P. Colombini, M. Orlando, F. Modugno, E. –L. Tolppa, M. Sardelli, L. Zoia and C. Crestini, *Microchem. J*. 2007, **85**, 164–173.

14 M. Bardet, M. F. Foray and T. Quoc-Troi, *Anal. Chem*. 2002, **74**, 4386–4390.

15 H. Yang, Y. Huaang, Q. Leng, B. A. Lepage and C. J. Williams, *Rev. Paleobot. Palinol*. 2005, **134**, 237–256.

16 F. Gugerli, L. Parducci and R. J. Petit, *New Phytol*. 2005, **166**, 409–418.

17 CBOL Plant Working Group. *PNAS* 2009**, 106**, 12794–12797.

18 I. Bruni, A. Galimberti, L. Caridi, D. Scaccabarozzi, F. De Mattia, M. Casiraghi and M. Labra, *Food Chem*. 2015, **170**, 308**–**315.

19 M. M. –Y. Tin, E. P. Economo and A. S. Mikheyev, *PLoS ONE* 2014, **9**, e96793.

20 R. Singh, Geetanjali and S. M. S. Chauhan, *Chem. Biodiv*. 2004, **1**, 1241–1264.

21 V. Cheynier, *Phytochem. Rev*. 2012, **11**, 153–177.

22 K. Venkataraman, *Phytochem*. 1972, **11**, 1571**–**1586.

23 T. Umezawa, *Phytochem. Rev*. 2003, **2**, 371–390.

24 J. Ralph, K. Lundquist, G. Brunow, F. Lu, H. Kim, P. F. Schatz, J. M. Marita, R. D. Hatfield, S. A. Ralph, J. H. Christensen and W. Boerjan, *Phytochem. Rev*. 2004, **3**, 29–60.

25 J. Vacek, J. Ulrichová, B. Klejdus and V. Šimánek, *Anal. Methods* 2010, **2**, 604–613.

26 F. Scholz and B. Meyer, *Electroanalytical Chemistry, A Series of Advances* 1998, **20**, 1–86.

27 F. Scholz, U. Schröder, R. Gulabowski and A. Doménech-Carbó, *Electrochemistry of Immobilized Particles and Droplets, 2nd edit*. Springer, Berlin-Heidelberg, 2014.

28 A. Doménech-Carbó, J. Labuda and F. Scholz, *Pure Appl. Chem.* 2013, **85**, 609–631.

29 A. Doménech-Carbó, M. T. Doménech-Carbó and V. Costa, *Electrochemical Methods in Archaeometry, Conservation and Restoration*. Monographs in Electrochemistry Series, F. Scholz, Edit. Springer, Berlin-Heidelberg, 2009.

30 A. Doménech-Carbó, *Anal. Methods* 2011, **3**, 2181–2188.

31 B. Cottyn, M. Rivard, A. Majira, J. Beauhaire, F. Allais, T. Martens, S. Baumberger and P. –H. Ducrot, *Phytochem. Lett*. 2015, **13**, 280–285.

32 G. Milczarek, *Electrochim. Acta* 2009, **54**, 3199–3205.

33 S. Admassie, T. Y. Nilsson and O. Inganäs, *Phys. Chem. Chem. Phys.* 2014, **16**, 24681–24684.

34 P. A. Kilmartin and C. F. Hsu, *Food Chem*. 2003, **82**, 501–512.

35 M. –E. Ghica and A. M. Oliveira-Brett, *Electroanalysis* 2005, **17**, 313–318.

36 A. K. Timbola, C. D. de Souza, C. Giacomelli and A. Spinelli, *J. Braz. Chem. Soc.* 2006, **17**, 139–148.

37 A. Masek, E. Chrzescijanska and M. Zaborski, *Food Chem*. 2014, **148**, 18–23.

38 T. Grygar, S. Kucková, D. Hradil and D. Hradilová, *J. Solid State Electrochem*. 2003, **7**, 706–713.

39 A. Doménech-Carbó, M. T. Doménech-Carbó and M. C. Saurí-Peris, *Talanta* 2005, **66**, 769–782.

40 P. Janeiro and A. M. Oliveira-Brett, *Electroanalysis* 2005, **17**, 733–738.

41 I. Novak, M. Seruga and Š. Komorsky-Lovrić, *J. Electroanal. Chem*. 2009, **631**, 71–75.

42 I. Novak, M. Seruga and Š. Komorsky-Lovrić, *Electroanalysis* 2009, **21**, 1019–1025.

43 A. Doménech-Carbó, M. T. Doménech-Carbó, M. Calisti and V. Maiolo, *Talanta* 2010, **81**, 404–414.

44 A. Doménech-Carbó, M. T. Doménech-Carbó, M. Calisti and V. Maiolo, *J. Solid State Electrochem*. 2010, **14**, 465-467.

45 Š. Komorsky-Lovrić and I. Novak, *Electrochim. Acta* 2013, **98**, 153–156.

46 Š. Komorsky-Lovrić and I. Novak, *Collect. Czech. Chem. Commun*. 2009, **74**, 1467–1475

47 Š. Komorsky-Lovrić and I. Novak, *J. Food. Sci*. 2011, **76**, C916–C920

48 M. Martini, L. M. De Carvalho, A. Blasco-Blasco and A. Doménech-Carbó, *Anal. Methods* 2015, **7**, 5740–5747.

49 I. Domínguez and A. Doménech-Carbó, *Sens. Actuat. B* 2015, **210**, 491–499.

50 A. Otto and V. Wilde, *Botan. Rev.* 2001, **67**, 141–238.

51 A. Otto, B. R. Simoneit and V. Wilde, *Botan. J. Linnean Soc.* 2007, **154**, 129–140.

52 M. Havelcová, Y. Sýkorová, A. Bechtel, K. Mach, H. Trejtnarová, M. Žaloudková, P. Matysová, J. Blažek, J. Boudová and J. Sakala, *Int. J. Coal Geol.* 2013, **107**, 62-77.

53 M. Scampicchio, S. Mannino, J. Zima and J. Wang, *Electroanalysis* 2005, **17**, 1215–1221.

54 A. Domenech-Carbó, A. Ibars, J. Prieto-Mossi, E. Estrelles, F. Scholz, G. Cebrián-Torrejón and M. Martini, *New J.Chem*. 2015, **39**, 7421–7428.

55 A. S. Ortiz-Miranda, P. König, H. Kahlert, F. Scholz, L. Osete-Cortina, M. T. Doménech-Carbó and A. Doménech-Carbó, *Anal. Bioanal. Chem.* 2016, **408**, 4943–4952.

Table 1. Identification of taxonomic units of wood samples in this study. [a] Repository of the Universitat Politècnica de València, [b] Prehistory Museum of Valencia.

Sample	Description	Anthracological identification	Electrochemical identification
S1	Study desk, anonymous, 17th-18th century (Oaxaca, Mexico)[a]	*Quercus robur*	*Quercus robur*
S2	*Retaule de San Pere*, anonymous, 14th century, (Cinctorres (Castellón), Spain)[a]	*Pinus sylvestris*	*Pinus sylvestris*
S3	Coffered ceiling of the *Igreja do Salvador*, anonymous, 14th century (Coimbra, Portugal)[a]	*Quercus pyrenaica*	*Quercus pyrenaica*
S4	Coffered ceiling of the *Lonja* building, (1503) (Valencia, Spain)[a]	*Pinus*	*Pinus*
S5	*Fascistol* of *Tlacochahuaya* church, anonimous, 17th-18th century (Oaxaca, Mexico)[a]	Conifer	Conifer
S6	*Retaule de la Verge de Gràcia, Sant Miquel Arcángel* church (Enguera (Valencia), Spain), Paolo de San Leocadio, 1482-1484[a]	*Pinus sylvestris*	*Pinus sylvestris*
S7	*Taules de Sant Vicent, Sant Jaume* church (Algemesí (Valencia), Spain Valencia), Francisco Ribalta, 1603-1605[a]	*Pinus* tp. *sylvestris*	*Pinus sylvestris*
S8	*Retaule de les Ànimes, Sant Martí* church (Sogorb (Castellón), Spain), workshop of Francisco Pérez, ca. 1625[a]	*Pinus halepensis*	*Pinus halepensis*
S9	*Retaule de Santa Úrsula, Sant Martí* church (Sogorb (Castellón) Spain), workshop of Francisco Pérez, ca. 1625[a]	*Pinus* tp. *halepensis*	*Pinus* tp. *halepensis*
S10	Cross, *San Cristobal Mártir* church (Picassent (Valencia), Spain), 18th-19th century (#45001)[b]	*Taxus baccata*	*Taxus*
S11	Arm from a scultpure, *San Cristobal Mártir* church (Picassent (Valencia), Spain), 18th-19th century (#45002)[b]	*Pinus* tp. *halepensis*	*Pinus* tp. *halepensis*
S12	Sculpture *San Cristobal Mártir* church (Picassent (Valencia), Spain), 18th-19th century (#45000)[b]	*Cedrus*	*Cedrus*

S13	Fragment of door, *Bastida de les Alcusses* (Moixent (Valencia), Spain), 375-350 BC (#1054-92) [b]	Conifer	*Pinus*
S14	Fragment of iron, *Bastida de les Alcusses* (Moixent (Valencia), Spain), 375-350 BC (#1054-119) [b]	*Pinus halepensis*	*Pinus halepensis*
S15	Shield *Bastida de les Alcusses* (Moixent (Valencia), Spain), 375-350 BC (#30.454) [b]	*Salix or Populus*	*Salix*

Figures

Figure 1. Photographs of regions of altarpieces **S7** (a, *Taules de Sant Vicent, Sant Jaume* church, Algemesí (Valencia), Spain, workshop of Francisco Ribalta, 1603-1605) and **S8** (b, *Retaule de les Ànimes, Sant Martí* church, Sogorb (Castellón), Spain, workshop of Francisco Pérez, ca. 1625). In the first case, sampling was allowed in the fractured region whereas in the second, almost all accessible wood surface area was covered by ground layers of the golden panel covering the wooden structure. Microscopy images of the c) radial and d) cross sections of sample **S7**. The arrow marks the region where sample **S7** was taken. Optical microscopy images (diascopic illumination, parallel polarized light) of the radial section of samples c) **S7** and d) **S6**. It can be seen that large pinoid pits occupied practically the entire cross-field.

Figure 2. a,b) CVs and c,d) their semi-derivative convolution, of microparticulate films deposited on GCE of a,c) ethanolic and b,d) acetone extracts of *Quercus robur* immersed into air-saturated 0.25 M aqueous acetate buffer, pH 4.75. Potential scan initiated at 0.0 V in the positive direction; potential scan rate 50 mV s^{-1}.

Figure 3. HPLC/MS of ethanolic extracts of a) *Quercus robur* and b) *Prunus avium*.

Figure 4. LSVs, after semi-derivative deconvolution, of ethanolic extracts of: a) *Ulmus glabra* (Urticales, Urticaceae); b) *Quercus petrae* (Fagales, Fagaceae); c) *Taxus baccata* (Pinales, Taxaceae); d) *Prunus avium* (Rosales, Rosaceae) in contact with aqueous acetate buffer. Potential scan initiated at 0.0 V in the positive direction; potential scan rate 50 mV s^{-1}.

Figure 5. Scheme for the electrochemical oxidation processes of a) syringic acid and b) baicalein.

Figure 6. a) FESEM image of a radial section of *Pinus* tp. *halepensis* from the church of San Cristóbal Mártir, Picassent (sample **S11**), Valencia and b-d) SWVs of microparticulate deposits from ethanolic extracts of: b) *Pinus halepensis* (black), sample **S11** (red) and sample **S14** (green); c) *Taxus baccata* (blanck) and sample **S10** (red); d) *Pinus sylvestris* (black), sample **S6** (red) and sample **S7** (green). Potential scan initiated

at –0.85 V in the positive direction; potential step increment 4 mV; square wave amplitude 25 mV; frequency 5 Hz.

Figure 7. Representation of $i(800)/i(\max)$ vs. $i(450)/i(\max)$ determined in LSVs, after semi-derivative convolution, of wood ethanolic extracts deposited on GCE in contact with aqueous acetate buffer for several families in this study. Potential scan initiated at 0.0 V in the positive direction; potential scan rate 50 mV s^{-1}. Data for three replicate experiments for each species are represented.

Figure 8. LSVs, after semi-derivative deconvolution, of microparticulate films of ethanolic extracts of: a) *Quercus robur*; b) *Quercus pyrenaica*; c) sample **S1**; d) sample **S3** immersed into air-saturated 0.25 M aqueous acetate buffer, pH 4.75. Potential scan initiated at 0.0 V in the positive direction; potential scan rate 50 mV s^{-1}.

Figure 9. Graphical matching between two normalized voltammograms A and B; representation of a,b) $I(E)_A$ vs. $I(E)_B$ and c,d) $[I(E)_A - I(E)_B]^2$ vs. E for a,c) A = *Quercus robur*, B = sample **S3**; b,d) A = *Fagus sylvatica*, B = sample **S3**. From LSVs of ethanolic wood extracts in contact with aqueous acetate buffer, conditions such as in Figures 3 and 7. Dotted lines represent the theoretical graphs for the case of perfect matching.

Figure 1.

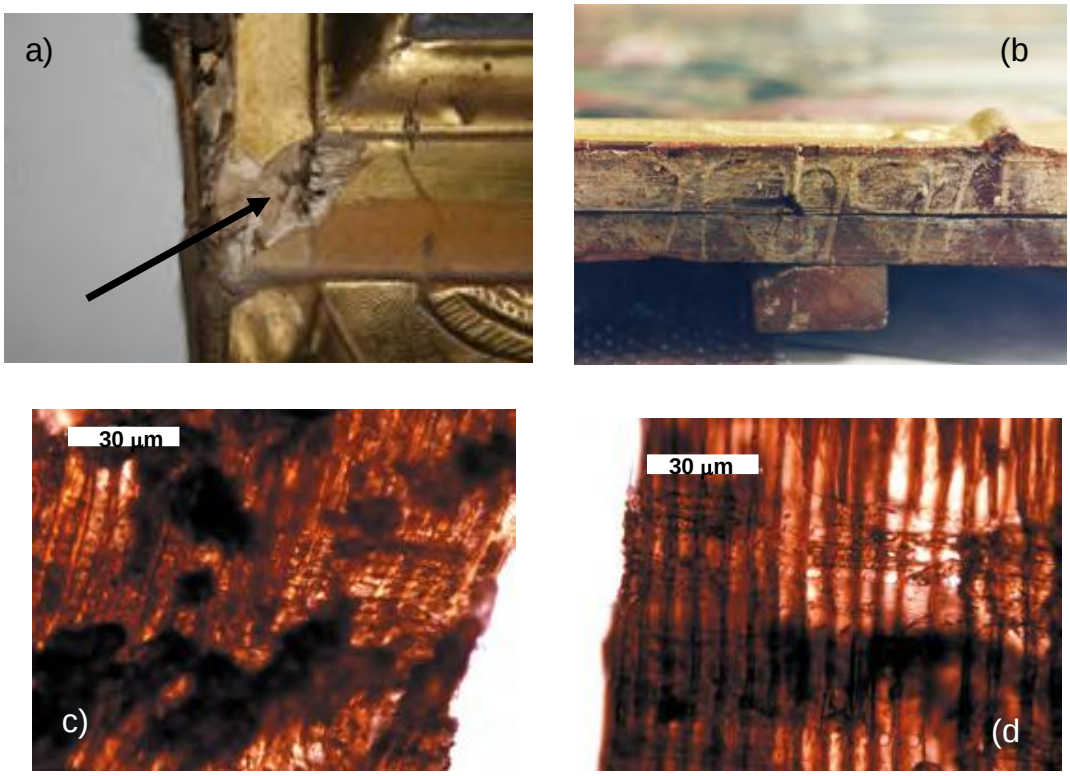

Figure 2.

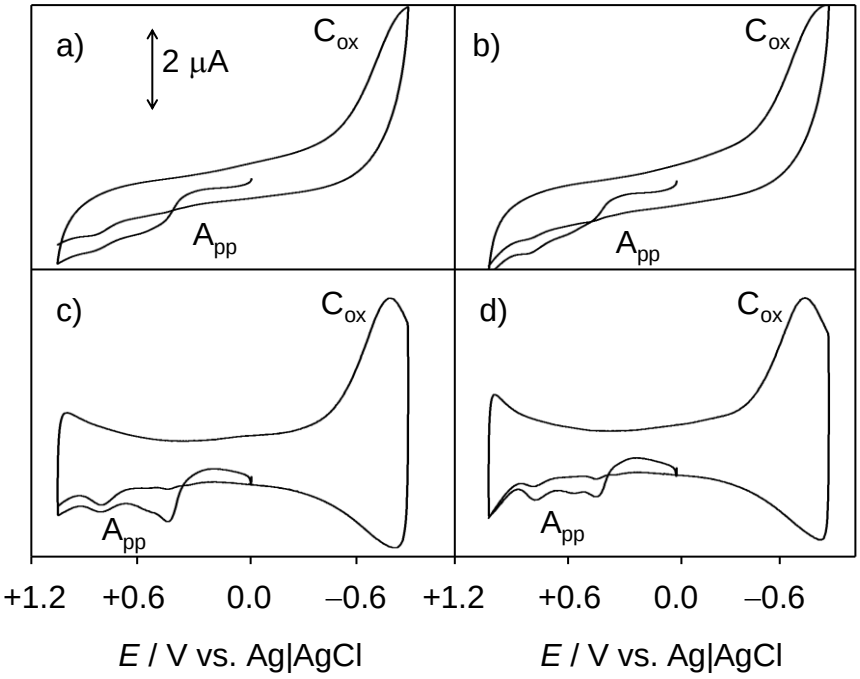
a)
2 μA
C_{ox}
A_{pp}
b)
C_{ox}
A_{pp}
c)
C_{ox}
A_{pp}
d)
C_{ox}
A_{pp}
+1.2 +0.6 0.0 –0.6 +1.2 +0.6 0.0 –0.6
E / V vs. Ag|AgCl
E / V vs. Ag|AgCl

Figure 3.

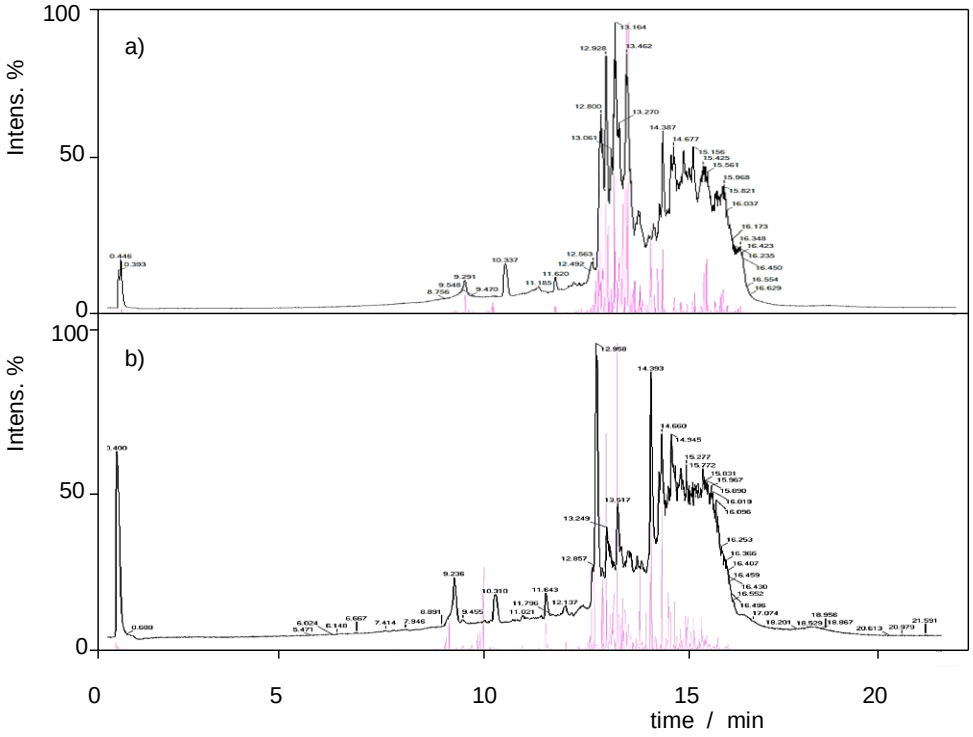

Figure 4.

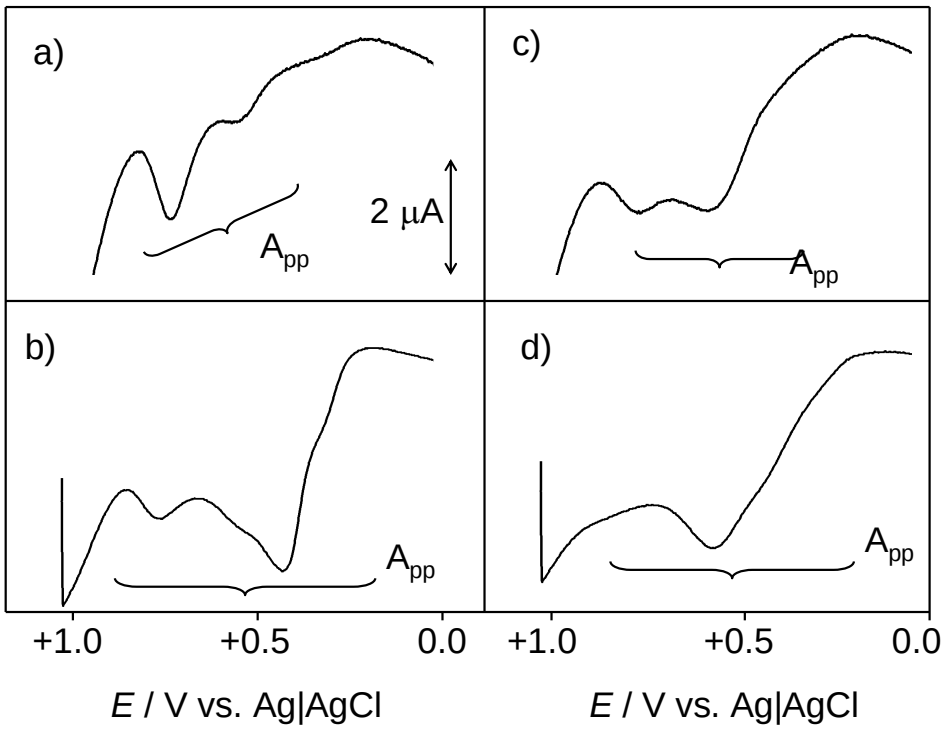
a)
2 µA
A_{pp}
c)
A_{pp}
b)
A_{pp}
d)
A_{pp}
+1.0
+0.5
0.0
+1.0
+0.5
0.0
E / V vs. Ag|AgCl
E / V vs. Ag|AgCl

Figure 5.

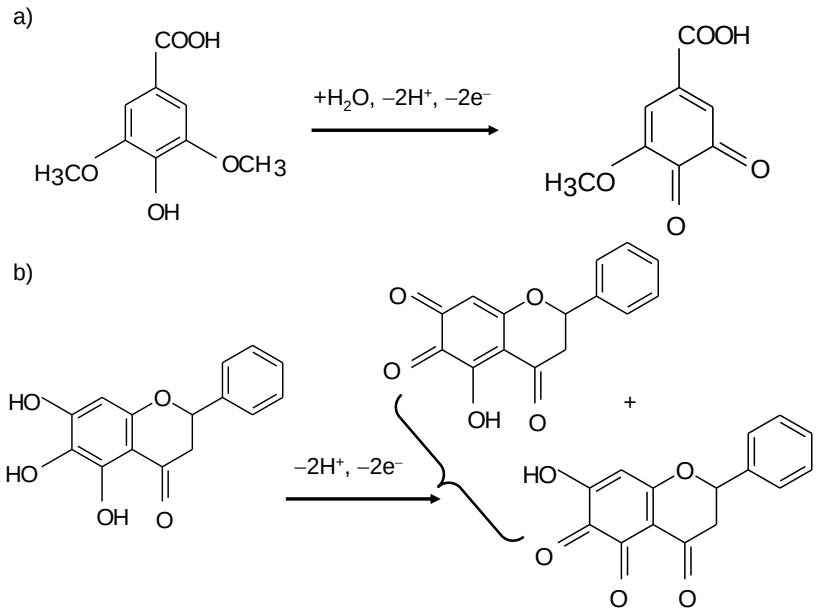
a)
COOH
H3CO
OCH3
OH
+H2O, –2H+, –2e–
COOH
H3CO
O
O
b)
HO
HO
OH
O
O
O
O
OH
O
+
–2H+, –2e–
HO
O
O
O
O

Figure 6.

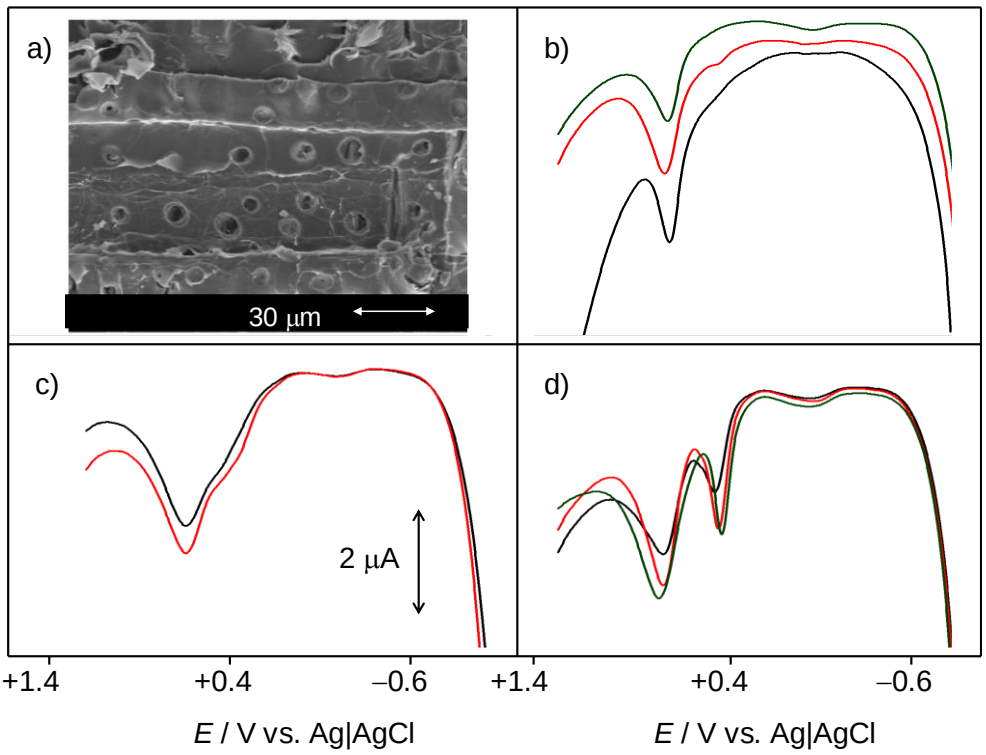

Figure 7.

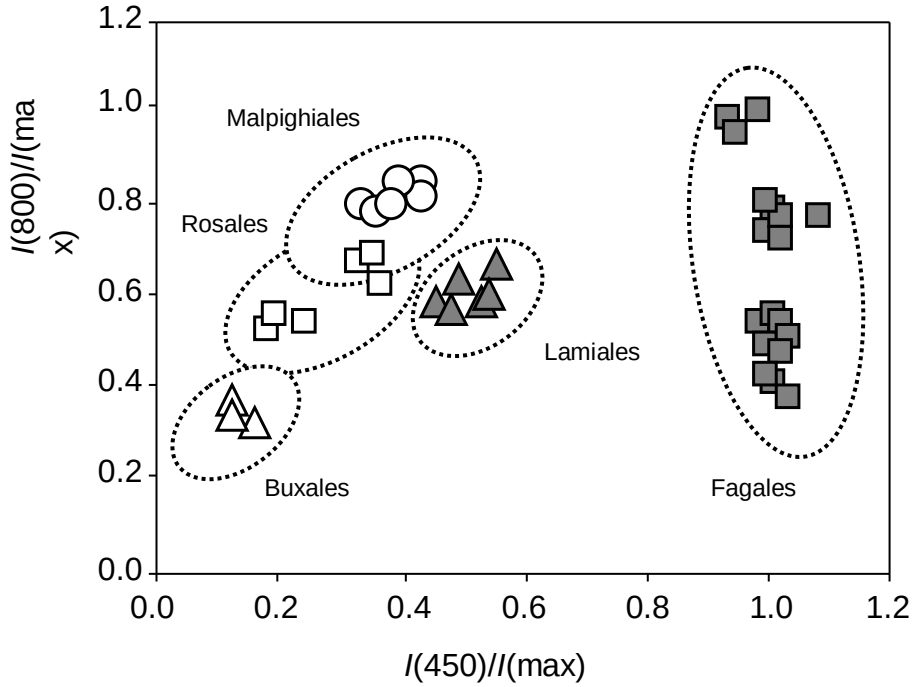
1.2
1.0
0.8
0.6
0.4
0.2
0.0
I(800)/I(max)
Malpighiales
Rosales
Lamiales
Buxales
Fagales
0.0
0.2
0.4
0.6
0.8
1.0
1.2
I(450)/I(max)

Figure 8.

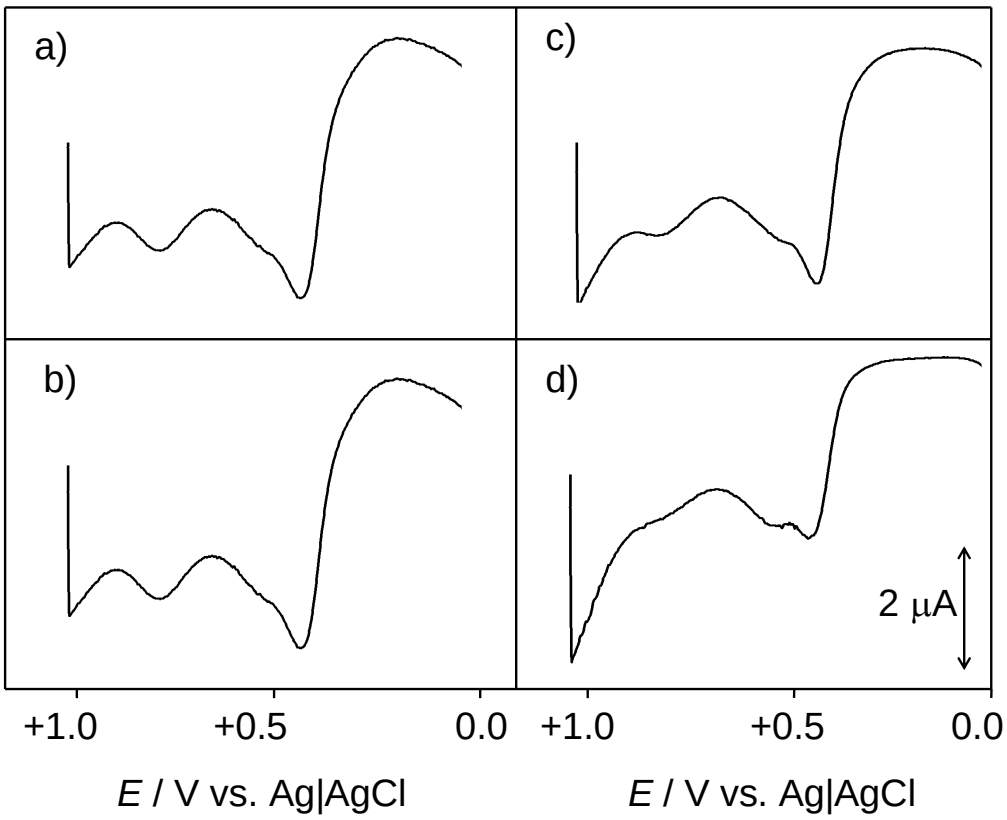

Figure 9.

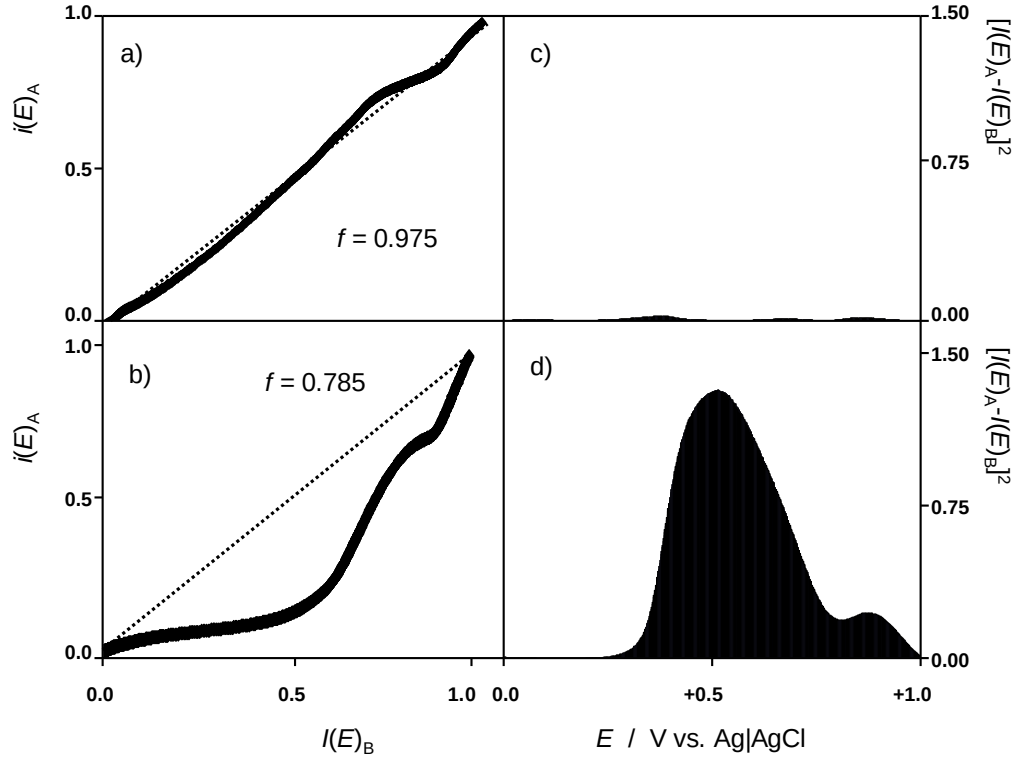
a)
b)
c)
d)
f = 0.975
f = 0.785
i(E)A
I(E)B
E / V vs. Ag|AgCl
[I(E)A-I(E)B]2
1.0
0.5
0.0
1.50
0.75
0.00
+0.5
+1.0